Probabilistic LMP Forecasting Considering Load Uncertainty

Article *in* IEEE Transactions on Power Systems · September 2009

DOI: 10.1109/TPWRS.2009.2023268 · Source: IEEE Xplore

CITATIONS
99

READS
291

2 authors:

Rui Bo
Missouri University of Science and Technology
73 PUBLICATIONS **1,113** CITATIONS

SEE PROFILE

Fangxing Li
University of Tennessee
328 PUBLICATIONS **6,530** CITATIONS

SEE PROFILE

Probabilistic LMP Forecasting Considering Load Uncertainty

Rui Bo, *Student Member, IEEE*, and Fangxing Li, *Senior Member, IEEE*

***Abstract*—In power market studies, the forecast of locational marginal price (LMP) relies on the load forecasting results from the viewpoint of planning. It is well known that short-term load forecasting results always carry certain degree of errors mainly due to the random nature of the load. At the same time, LMP step changes occur at critical load levels (CLLs). Therefore, it is interesting to investigate the impact of load forecasting uncertainty on LMP. With the assumption of a certain probability distribution of the actual load, this paper proposes the concept of probabilistic LMP and formulates the probability mass function of this random variable. The expected value of probabilistic LMP is then derived, as well as the lower and upper bound of its sensitivity. In addition, two useful curves, alignment probability of deterministic LMP versus forecasted load and expected value of probabilistic LMP versus forecasted load, are presented. The first curve is designed to identify the probability that the forecasted price in a deterministic LMP matches the actual price at the forecasted load level. The second curve is demonstrated to be smooth and therefore eliminates the step changes in deterministic LMP forecasting. This helps planners avoid the possible sharp changes during decision-making process. The proposed concept and method are illustrated with a modified PJM five-bus system and the IEEE 118-bus system.**

***Index Terms*—Critical load level, energy markets, load forecasting, locational marginal pricing (LMP), normal distribution, optimal power flow (OPF), power markets, probabilistic LMP forecasting, uncertainty.**

I. Introduction

PREDICTION of load, especially short-term load consumption, has long been an important topic in academia and industrial research and practices [1]. With the deregulation of power industry and the adoption of locational marginal pricing (LMP) methodology, LMP forecasting has attracted lots of attentions because of the significance of LMP in delivering market price signals and being used for settlement [2]–[4].

It is known that LMP can be decomposed into three components with each representing the marginal energy price, marginal loss price, and marginal congestion price, respectively [5]–[7]. The decisive factors of LMP include supply bids, demand offers, load forecasting, and network topology. In a day-ahead power market, once the market is closed (for example at 12:00 noon before the operating day), the offers and bids are fixed and a transmission network model will be used in day-ahead market scheduling. Nevertheless, load remains uncertain because there is essentially no way to discover the exact load of each hour of the next operating day. Load forecasting is applied to address this issue, but performance varies with models, algorithms and the nature of the problem. It is apparent that the uncertainty associated with load directly leads to the uncertainty of LMP. Therefore, as equally important as the study of other economic impact of load forecasting [8]–[11], it is necessary to investigate how the LMP will be affected by uncertainty of load, or, uncertainty of load forecasting results in practice.

Optimal power flow (OPF) problem has been discussed in [12] with special attention to computational issues brought by deregulation. A methodology of computing LMP sensitivities with respect to load in ac optimal power flow (ACOPF) framework has been presented in [13]. Approaches for dc optimal power flow (DCOPF) have been applied in [6], [14], and [15]. In [15], a perturbation-based algorithm is proposed to identify the next critical load level (CLL), defined as a load level at which an LMP step change, as well as the change of binding and unbinding limits, occurs. This algorithm is demonstrated to be very computationally efficient since it does not require multiple optimization runs. It essentially enables the efficient study of LMP on any range of load variations.

Fig. 1 shows a typical LMP versus load curve [14], [15] for a sample system slightly modified from the original PJM five-bus system defined in [16]. Losses are ignored in those studies such that this research is concentrated on the overall behavior of LMP due to congestions. In theory, the horizontal axis denotes the actual load. In practice, the axis represents the forecasted load, since forecasted load is utilized to perform dispatch and LMP calculation.

It can be seen that there is a step change of LMP when load increases to a CLL, e.g., the load level at 600 MW, 640 MW, 711.81 MW, etc. At each CLL, a new binding limit, either a transmission line thermal limit or a generator capacity limit, occurs. Meanwhile, there is a change of the marginal unit set and marginal generation sensitivity with respect to load, which results in the LMP step change.

At CLLs, LMP is highly sensitive and the sensitivity of LMP with respect to load is evaluated as infinite mathematically. This step change characteristic of LMP leads to the ambiguity of LMP evaluation at CLLs. For example, when forecasted load happens to be 711.81 MW, there are at least two choices to set price at bus D: \$15.00/MWh or \$31.46/MWh. But it is not well

Manuscript received December 04, 2008; revised January 31, 2009. First published July 10, 2009; current version published July 22, 2009. Paper no. TPWRS-00895-2008.

The authors are with the Min H. Kao Department of Electrical Engineering and Computer Science, The University of Tennessee, Knoxville, TN 37996 USA (e-mail: fli6@utk.edu).

Color versions of one or more of the figures in this paper are available online at http://ieeexplore.ieee.org.

Digital Object Identifier 10.1109/TPWRS.2009.2023268

justified which one should be taken. Taking into account the load variation direction (namely, increase or decrease) may be an option.

A more important impact of this step change is that slight difference in forecasted load may result in dramatic difference in LMP. For example, LMP at bus D is \$15.00/MWh when forecasted load is 711.80 MW whereas the price soars to \$31.46/MWh when forecasted load is slightly off by 0.1 MW, making it 711.90 MW. On the other hand, it is very likely for a load forecasting tool, even well-tuned, to produce a result with an error greater than 0.1 MW for a target load around 700 MW level. Therefore, load forecasting uncertainty may significantly affect LMP forecasting and, consequently, market participants' financial or bidding decision.

There are a few reasons leading to the uncertainty of load forecasting result. First of all, future load is a random variable indeed and cannot be predicted accurately. Each load forecasting method has its own theoretical foundations and likely produces results different from others. Each method may excel in certain applications, but no one can achieve 100% accuracy. There is always a certain error range associated with the forecasted results. Second, even for the same method, the results may be different by using different settings, tunings and assumptions. Last, most methods suffer from missing data and highly rely on the input data accuracy.

Although the uncertainty in load forecast is unavoidable, the load forecasting errors are often described by certain probability distribution, which enables the study of the correlation between forecasted load and LMP in a probabilistic sense. The LMP study considering probabilistic factors has been presented in [17] and [18] by modeling generator biddings as stochastic variables. However, there is no existing research work to specifically investigate the impact of load forecast uncertainty on LMP simulation results for price forecast purpose. We intend to reveal the probabilistic aspect of the traditional LMP with respect to load uncertainty and present useful information such as the likelihood that a forecasted deterministic LMP will occur. This helps generation companies or load serving entities formulate their bidding strategies, risk hedging policies, and even long-term contract negotiation. More importantly, this paper systematically presents the concept of probabilistic LMP from the viewpoint of forecasting, and indicates that the forecasted probabilistic LMP should be a set of discrete values with associated probabilities at different load intervals. These two aspects are the motivation and significance of this paper.

This paper is organized as follows. Section II introduces the assumptions upon which the research relies, proposes the concept of probabilistic LMP and formulates the probability mass function of this random variable, as well as the alignment probability of deterministic LMP versus forecasted load curve. Section III presents the formulation of the expected value of probabilistic LMP, shows the sensitivity bounds, and presents an approximate approach to calculate probabilistic LMP. Sections IV and V present results from a modified PJM five-bus system and the IEEE 118-bus system, respectively. Section VI summarizes the paper and points out possible future work.

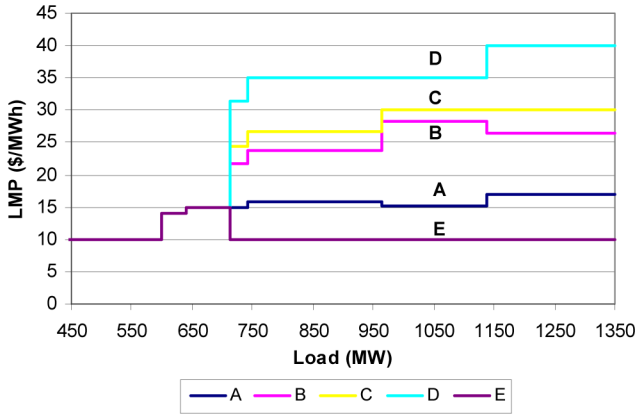

Fig. 1. LMP at all buses with respect to different system loads for the modified PJM five-bus system.

II. Probabilistic LMP and Its Probability Mass Function

A. Assumptions

Actual load, or load forecasting error, can be assumed to be a random variable and follow certain probability distribution. However, it is difficult to determine the distribution type due to insufficient historical data [10]. Normal distribution is a frequently used candidate and has been employed to model actual load in a number of research works [8]–[11], and therefore will be used in this paper to describe the actual load at hour t. Then, we have

$$D_t \sim N(\mu_t, \sigma_t^2) \tag{1}$$

$$\varphi(x) = \frac{1}{\sigma_t\sqrt{2\pi}} e^{-\frac{(x-\mu_t)^2}{2\sigma_t^2}} \tag{2}$$

$$\Phi(x) = \int_{-\infty}^{x} \varphi(u)du \tag{3}$$

where

$D_t =$ a random variable for the actual load at hour t;
N denotes normal distribution;
$\mu_t =$ mean of D_t;
$\sigma_t^2 =$ variance of D_t;
$\varphi(x) =$ probability density function of D_t;
$\Phi(x) =$ cumulative density function of D_t.

It should be emphasized that for a well-tuned load forecasting model, the forecasted load at hour t, D_t^F, should be very close to the mean value of D_t, i.e., μ_t. However, D_t^F is also deemed not to be exactly equal to μ_t due to the error of load forecasting. Nevertheless, it is a common practice in market simulation or forecast to use a single forecasted value of load (D_t^F) to perform a deterministic market simulation to forecast LMP, congestion, etc. There is no reported research work to incorporate load forecasting uncertainty into LMP simulation and price forecasting. This explains the novelty of this research work.

B. Models for the LMP-Load Curve

As the random variable D_t is represented by the horizontal axis, the LMP-load curve (similar to the curves in Fig. 1) is illustratively redrawn in Fig. 2 to facilitate the following study.

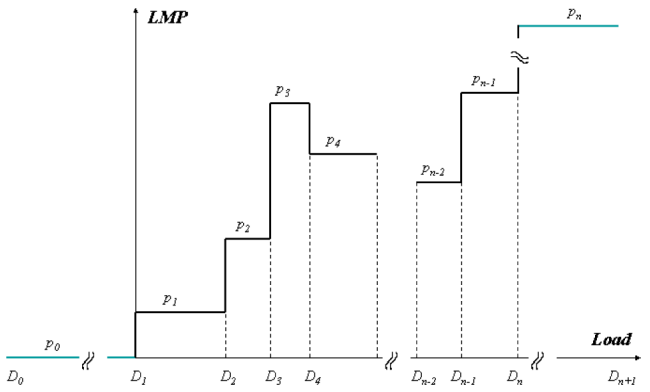

Fig. 2. Extended LMP versus load curve.

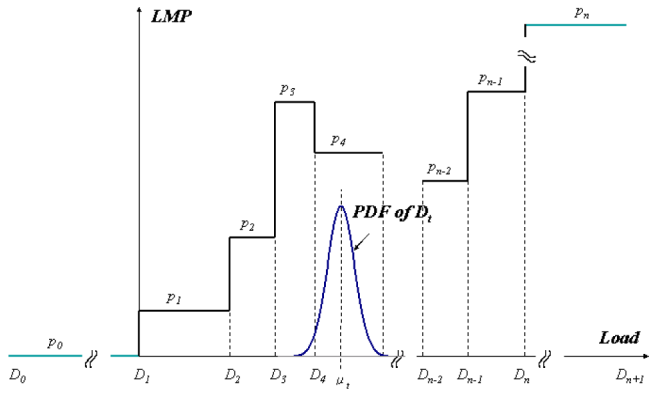

Fig. 3. LMP-load curve and probability distribution of D_t.

As shown in Fig. 2, the load axis is divided into $n-1$ segments by a sequence of CLLs, $\{D_i\}_{i=1}^{n}$. Here D_1 represents no-load case (i.e., $D_1 = 0$), and D_n represents the maximum load that the system can supply due to the limits of total generation resources and transmission capability. Associated with each load segment i, there is a corresponding actual LMP value, p_i, which is considered a constant in this study as we ignore loss model for simplicity. The model to calculate LMP without losses, which is used in this work, can be found in many previous works such as in the introductory part in [14].

The LMP-load curve in Fig. 2 includes two extra segments. One is for load from D_0 to D_1, where D_0 denotes negative infinite load, and the associated price, p_0, is zero. The second additional segment is defined as the load range from D_n to D_{n+1}, where D_{n+1} represents positive infinite load. In this segment the price is set to be value of lost load (VOLL) to reflect demand response to load shedding. Although VOLL varies with customer groups and load interruption time and duration, it is a common practice to get an aggregated VOLL to represent the average loss for an area. Therefore, VOLL is assumed to be a constant value for simplicity in this paper.

The two extra segments are added for mathematical completeness. In fact, they have trivial, if not none, impact on the study because the typical load range under study (for instance, from 0.8 p.u. to 1.2 p.u. of an average case load) is far from these two extreme segments, and the possibility of having forecasted load close to zero or greater than D_n, the maximum load that the system can supply, is extremely rare and numerically zero.

The curve can be formulated as

$$\mathrm{LMP}(D) = \begin{cases} p_0, & D_0 < D \le D_1 \\ p_1, & D_1 < D \le D_2 \\ \vdots & \\ p_{n-1}, & D_{n-1} < D \le D_n \\ p_n, & D_n < D \le D_{n+1} \end{cases} \tag{4}$$

where $p_0 = 0$, $p_n = \mathrm{VOLL}$, $D_0 = -\infty$, $D_1 = 0$, and $D_{n+1} = \infty$.

The compact representation is given as follows:

$$\mathrm{LMP}(D) = \{p_i | i \in \{0, 1, \ldots, n\}, D_i < D \le D_{i+1}\}. \tag{5}$$

Apparently, $(\partial \mathrm{LMP})/(\partial D)$, the LMP sensitivity with respect to load, is infinite at the CLLs, $\{D_i\}_{i=1}^{n-1}$.

C. Probabilistic LMP and Its Probability Mass Function

Here it is assumed that economic dispatch and LMP calculation are performed on an hourly basis. LMP at hour t, denoted by LMP_t, is a function of D_t which is a random variable from the viewpoint of forecasting. Therefore, at the forecasting or planning stage, LMP_t should be viewed as a random variable too and this characteristic is inherited from forecasted load. Fig. 3 shows the LMP-load curve and the probability distribution function (PDF) of D_t. It can be inferred from Fig. 3 that LMP_t should be a discrete random variable, with $n+1$ possible values denoted by the sequence $\{p_i\}_{i=0}^{n}$. Certainly, the probability that the actual price is aligned with different p_i will be different. The random variable LMP_t is named *probabilistic LMP* in this paper, in order to be differentiated from the traditionally deterministic LMP.

Furthermore, the probability that LMP_t has an actual value of p_i can be expressed as

$$\Pr(\mathrm{LMP}_t = p_i) = \int_{D_i}^{D_{i+1}} \varphi(u)du = \Phi(D_{i+1}) - \Phi(D_i). \tag{6}$$

The cumulative density function $\Phi(x)$ can be well estimated by available approximation methods to ease the computation [19]. A schematic graph of the probability mass function (PMF) of LMP_t is shown in Fig. 4. It should be pointed out that mathematically the PMF graph is usually presented in a way such that possible values are sorted in ascending order, and the probability of identical prices (for example when $p_i = p_j$ where $i \neq j$) are merged together. However, it is not done in Fig. 4 for the purpose of easy presentation. That is, Fig. 4 shows the PMFs in the order of the occurrence of the associated price, p_i, as load increases.

Equations (5) and (6) and Fig. 4 show the important characteristic of the concept of probabilistic LMP proposed in this paper:

> Probabilistic LMP at a specific (mean) load level is not a single deterministic value. Instead, it represents a set of discrete values at a number of load intervals. Each value has an associated probability.

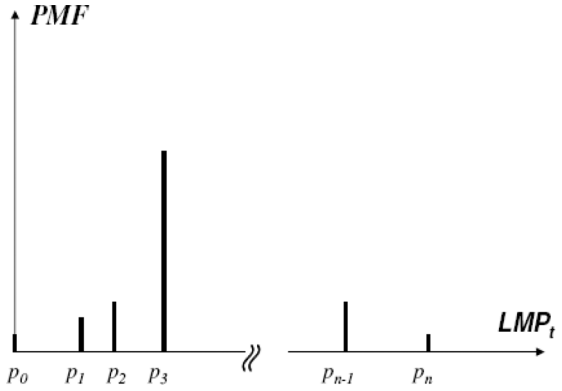

Fig. 4. Probability mass function of probabilistic LMP at hour t.

D. Alignment Probability of Deterministic LMP Forecasting Versus Forecasted Load Curve

At hour t, if a single value of forecasted load D_t^F is used for LMP forecasting, the calculated LMP can be deterministically identified by looking up the LMP-load curve as shown in Fig. 2. Suppose D_t^F is between D_j and D_{j+1}, then the corresponding $\mathrm{LMP}(D_t^F)$ is equal to p_j. This can be written as

$$\mathrm{LMP}(D_t^F) = p_j, \quad D_j < D_t^F \le D_{j+1} \tag{7}$$

where $\mathrm{LMP}(D_t^F)$ is the LMP corresponding to the forecasted load D_t^F. This can be called deterministic LMP forecast.

Then, the probability that the actual price LMP_t is the same as $\mathrm{LMP}(D_t^F)$, i.e., p_j, can be obtained from the PMF as shown in Fig. 4. It should be noted that the actual load may not be D_t^F, or not even in the range of $[D_j, D_{j+1}]$. Hence, the actual price is not always the same as the forecasted price. In a rigorous way, we define an alignment probability that the actual price is the same as forecasted price in a deterministic LMP forecasting. This can be written as

$$\begin{aligned}\mathrm{AP} &= \Pr\left(\mathrm{LMP}_t = \mathrm{LMP}\left(D_t^F\right)\right) = \Pr(\mathrm{LMP}_t = p_j) \\ &= \int_{D_j}^{D_{j+1}} \varphi(u)du = \Phi(D_{j+1}) - \Phi(D_j)\end{aligned} \tag{8}$$

where AP or $\Pr(\mathrm{LMP}_t = p_j)$ is the alignment probability in deterministic LMP forecasting. Apparently, the probability that the actual price is not the same as the forecasted price in a deterministic approach is equal to $1 - \Pr(\mathrm{LMP}_t = p_j)$ in general.

When the above equation is evaluated for every D_t^F in the entire interval $[D_1, D_n]$, an alignment probability versus D_t^F curve can be obtained. Each point of the curve represents the alignment probability that the projected $\mathrm{LMP}(D_t^F)$ is the actual price when the forecasted load is D_t^F. When combined with the LMP-load curve, this LMP alignment probability versus forecasted load curve delivers very useful information such as how likely the projected LMP, $\mathrm{LMP}(D_t^F)$ at the forecasting stage, is the same as the actual LMP at hour t, LMP_t.

The alignment probability defined in (8) gives the probability that the deterministically forecasted LMP and the actual LMP are exactly the same. This sometimes may not be fair if the actual LMP have a good chance, such as 70%, to give a price that is very close to, but not exactly the same as, the deterministic LMP result. With (8), they are not considered as aligned and the alignment probability will be as low as 30%. Hence, tolerance level can be applied to address this. For instance, if we choose 10% as the price tolerance level, then the result of the deterministically forecasted LMP is considered aligned with the actual LMP if the actual LMP is within [90%, 110%] of the deterministic LMP. Namely, we can define alignment probability with tolerance, AP_α, as

$$\mathbf{AP}_\alpha = \mathbf{Pr}(p_j \times (1-\alpha\%) \le \mathrm{LMP}_t \le p_j \times (1+\alpha\%)) \tag{9}$$

where α is the tolerance percentage. This gives the confidence of having LMP forecast in an acceptable range.

The above discussion will be further elaborated in the numeric studies.

III. Expected Value of the Probabilistic LMP

A. Expected Value of Probabilistic LMP

Since LMP at hour t, LMP_t, is a random variable, it is interesting to see the expected value of LMP at hour t:

$$\begin{aligned}E(\mathrm{LMP}_t) &= \sum_{i=0}^{n} \Pr(\mathrm{LMP}_t = p_i) \times p_i \\ &= \sum_{i=0}^{n} \left(\int_{D_i}^{D_{i+1}} \varphi(u)du \right) \times p_i \\ &= \sum_{i=0}^{n} p_i \times \int_{D_i}^{D_{i+1}} \frac{1}{\sigma_t\sqrt{2\pi}} e^{-\frac{(u-\mu_t)^2}{2\sigma_t^2}} du\end{aligned} \tag{10}$$

where $E(\cdot)$ is the expected value operator.

It can be seen that $E(\mathrm{LMP}_t)$ is a function of μ_t and σ_t. The function is defined as

$$E_{\mathrm{LMP}_t}(\mu_t, \sigma_t) \triangleq E(\mathrm{LMP}_t). \tag{11}$$

B. Expected Value of Probabilistic LMP Versus Forecasted Load Curve

If $E_{\mathrm{LMP}_t}(\mu_t, \sigma_t)$ is evaluated for every μ_t in the interval $[D_1, D_n]$, the expected value of probabilistic LMP versus μ_t curve will be obtained.

In practice, it is sometimes more interesting to see the expected value of probabilistic LMP with respect to forecasted load (D_t^F) curve since D_t^F, instead of μ_t, is actually available. If there is a constant deviation C_{dev} of D_t^F from μ_t (for instance due to model calibration error), namely, $D_t^F = \mu_t - C_{\mathrm{dev}}$, then $E_{\mathrm{LMP}_t}(D_t^F) = E_{\mathrm{LMP}_t}(\mu_t - C_{\mathrm{dev}})$. It implies that the expected value of probabilistic LMP versus D_t^F curve can be obtained by left-shifting the expected value of probabilistic LMP versus μ_t curve by C_{dev}. Likewise, if the deviation of D_t^F from μ_t is a constant portion r of μ_t, namely, $D_t^F = \mu_t(1-r)$, then $E_{\mathrm{LMP}_t}(D_t^F) = E_{\mathrm{LMP}_t}(\mu_t(1-r))$. It indicates that the expected value of probabilistic LMP versus D_t^F curve can be obtained by laterally scaling the expected value of probabilistic LMP versus μ_t curve by a factor of $(1-r)$ along μ_t axis. Therefore, in both cases, the shape of the expected value of probabilistic LMP versus D_t^F curve is similar to, if not the same as, that of expected value of probabilistic LMP versus μ_t curve. In general,

one curve can be obtained by simple geometrical operation on the other curve.

Furthermore, despite the possible difference between D_t^F and μ_t, it can be normally assumed that the forecasted load D_t^F is equal to μ_t as previously mentioned. Consequently, we have $E_{\mathrm{LMP}_t}(D_t^F) = E_{\mathrm{LMP}_t}(\mu_t)$. For notational convenience, this assumption is taken in the following study. Therefore, $E_{\mathrm{LMP}_t}(\mu_t)$ and $E_{\mathrm{LMP}_t}(D_t^F)$ are interchangeable, and so are μ_t and D_t^F.

It should be noted that $E_{\mathrm{LMP}_t}(\mu_t, \sigma_t)$ is continuously differentiable at μ_t. Therefore, the sensitivity of expected value of probabilistic LMP with respect to μ_t can be derived using the theory of parametric derivative of integration, which is stated as follows.

If $f(x, y), f_x(x, y)$ are continuous on $[a, b] \times [c, d]$, then the derivative of $I(x) = \int_c^d f(x, y)dy$ is continuous, and $I'(x) = \int_c^d f_x(x, y)dy$.

By this theory, the sensitivity of probabilistic LMP is derived as

$$\begin{aligned}\frac{\partial E_{\mathrm{LMP}_t}(\mu_t, \sigma_t)}{\partial \mu_t} &= \sum_{i=0}^{n} p_i \times \int_{D_i}^{D_{i+1}} \left(\frac{1}{\sigma_t \sqrt{2\pi}} e^{-\frac{(u-\mu_t)^2}{2\sigma_t^2}} \right) \times \frac{2(u-\mu_t)}{2\sigma_t^2} du \\ &= \sum_{i=0}^{n} p_i \times \int_{D_i}^{D_{i+1}} \frac{u-\mu_t}{\sigma_t^3 \sqrt{2\pi}} e^{-\frac{(u-\mu_t)^2}{2\sigma_t^2}} du. \end{aligned} \tag{12}$$

Equation (12) can be further derived as (13). Details of the derivation are included in Appendix A:

$$\begin{aligned}\frac{\partial E_{\mathrm{LMP}_t}(\mu_t, \sigma_t)}{\partial \mu_t} &= \frac{1}{\sigma_t \sqrt{2\pi}} \times \left[\sum_{i=1}^{n-1} p_i \times \left(e^{-\frac{(D_i-\mu_t)^2}{2\sigma_t^2}} - e^{-\frac{(D_{i+1}-\mu_t)^2}{2\sigma_t^2}} \right) \right. \\ &\quad \left. + p_n \times e^{-\frac{(D_n-\mu_t)^2}{2\sigma_t^2}} \right]. \end{aligned} \tag{13}$$

C. Lower and Upper Bound of Sensitivity of Expected Value of Probabilistic LMP

The absolute value of the sensitivity of expected value of probabilistic LMP has an upper bound as follows. The derivation is given in Appendix B:

$$\left| \frac{\partial E_{\mathrm{LMP}_t}(\mu_t, \sigma_t)}{\partial \mu_t} \right| \le \frac{1}{\sigma_t \sqrt{2\pi}} \sum_{i=1}^{n} |p_i|. \tag{14}$$

Therefore, $(\partial E_{\mathrm{LMP}_t}(\mu_t, \sigma_t))/(\partial \mu_t)$ has a finite lower and upper bound for a given nonzero σ_t:

$$\begin{aligned} -\frac{1}{\sigma_t \sqrt{2\pi}} \sum_{i=1}^{n} |p_i| &\le \frac{\partial E_{\mathrm{LMP}_t}(\mu_t, \sigma_t)}{\partial \mu_t} \\ &\le \frac{1}{\sigma_t \sqrt{2\pi}} \sum_{i=1}^{n} |p_i|. \end{aligned} \tag{15}$$

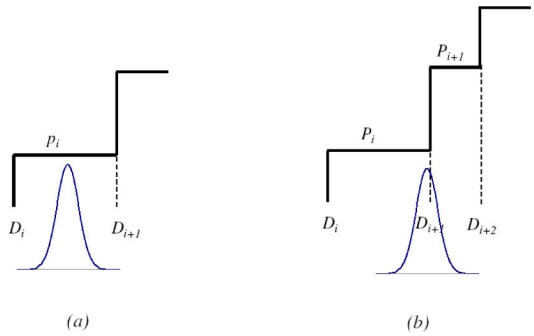

Fig. 5. Two cases of approximated calculation of expected value of probabilistic LMP. (a) $D_i + 3\sigma_t < \mu_t < D_{i+1} - 3\sigma_t$. (b) $D_i + 3\sigma_t < \mu_t < D_{i+2} - 3\sigma_t$.

Equation (15) implies that the upper bound increases when standard deviation goes smaller. An extreme case is when load forecast is completely accurate, namely, when σ_t is zero, then the upper bound is infinite. It implies that a step change may occur at this particular situation. This pattern will be exemplified in the numerical studies.

D. Approximate Calculation of Expected Value of Probabilistic LMP

The calculation of expected value of probabilistic LMP involves complicated mathematical integration; however, it can be simplified by applying certain approximation for some particular cases.

For normal distribution with mean μ and standard deviation σ, the ratio of the probability in $[\mu-3\sigma, \mu+3\sigma]$ to the probability outside this interval is

$$\frac{\Pr(\mu - 3\sigma < x < \mu + 3\sigma)}{\Pr(x < \mu - 3\sigma) + \Pr(x > \mu + 3\sigma)} \approx 384. \tag{16}$$

Therefore, even if the price of the interval outside $[\mu-3\sigma, \mu+3\sigma]$ is about 38.4 times higher than the price within the interval $[\mu - 3\sigma, \mu + 3\sigma]$, the possible impact to $E(LMP_t)$ from the interval outside $[\mu - 3\sigma, \mu + 3\sigma]$ will be less than 10%. Hence, we can ignore the impact of the interval outside $[\mu - 3\sigma, \mu + 3\sigma]$. Therefore, the expected value of probabilistic LMP under certain conditions, as shown in Fig. 5, can be approximated as follows:

a) if $D_i + 3\sigma_t < \mu_t < D_{i+1} - 3\sigma_t$, then

$$E(\mathrm{LMP}_t) \approx p_i.$$

b) if $D_i + 3\sigma_t < \mu_t < D_{i+2} - 3\sigma_t$, then

$$E(\mathrm{LMP}_t) \approx a \times p_i + b \times p_{i+1} \approx a \times p_i + (1-a) \times p_{i+1}$$

where

$$\begin{aligned} a &= \Phi(D_{i+1}) - \Phi(D_i) \approx \Phi(D_{i+1}) \\ b &= \Phi(D_{i+2}) - \Phi(D_{i+1}) \approx 1 - \Phi(D_{i+1}) = 1 - a. \end{aligned}$$

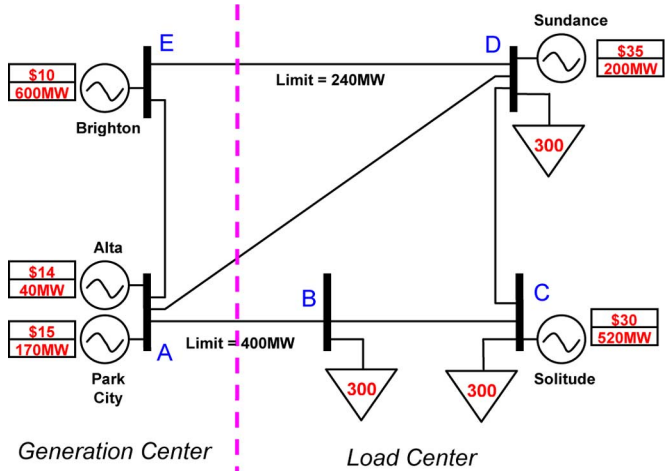

Fig. 6. Base case modified from the PJM five-bus system.

These approximations will be close enough to the actual values and meanwhile help to save computational efforts for the cases with broad range between CLLs. For example in Fig. 1, load in the range of (0 MW, 570 MW) falls into the case (a) category, and the expected value of probabilistic LMP could be easily calculated, which is essentially \$10/MWh throughout this interval.

Moreover, considering the fact that well-tuned commercial load forecasting tools are capable of generating fairly small amount of error, an analyst could focus on a narrow range around the forecasted load, such as two or three standard deviations. This could overcome the increases in computation for large market areas where much more LMP-load segments will appear due to multiple bid segments, more generators, and potentially more congested transmission lines.

IV. Numerical Study of a Modified PJM Five-Bus System

In this section, numeric study will be performed on the PJM five-bus system [16] with slight modification. The modifications are for illustration purpose and are detailed in [14]. Fig. 6 shows the configuration of the system.

To calculate the LMP versus load curve as shown in Fig. 1, it is assumed that the system load change is distributed to each bus load proportional to its base case load for simplicity. Therefore, the load change is equally distributed at Buses B, C, and D since each has 300 MW load in the base case. This is roughly reasonable because proportional distribution from area load to bus load is commonly used in industrial practices in planning, at least for conforming loads. Also, the proportional distribution is also used in continuation power flow for voltage stability study. It should be pointed out that the distribution pattern of system load variation could be modeled in a more sophisticated way [15]. Since this paper aims to illustrate the concept of probabilistic LMP considering load uncertainty, we use proportional variation pattern for simplicity. More complicate model such as considering conforming and nonconforming loads can be addressed in future work.

TABLE I
CLL and LMPs

CLL(MW)	LMP@A	LMP@B	LMP@C	LMP@D	LMP@E
0.00	10.00	10.00	10.00	10.00	10.00
600.00	14.00	14.00	14.00	14.00	14.00
640.00	15.00	15.00	15.00	15.00	15.00
711.81	15.00	21.74	24.33	31.46	10.00
742.80	15.83	23.68	26.70	35.00	10.00
963.94	15.24	28.18	30.00	35.00	10.00
1137.02	16.98	26.38	30.00	39.94	10.00
1484.06	16.98	26.38	30.00	39.94	10.00

Note: LMPs are all in the unit of \$/MWh; Prices at the gray boxes show LMP at bus B decreases when load increases.

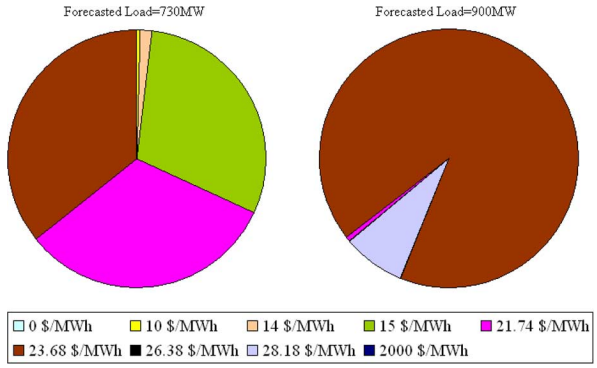

Fig. 7. PMF of LMP_t at Bus B.

The CLLs and the corresponding LMPs at each bus are shown in Table I. These data are the data source of Fig. 1 and are calculated by the efficient solver presented in [15].

For simplicity and better illustration, it is assumed that μ_t is always equal to forecasted load D_t^F, and the standard deviation σ_t is taken as 5% of the mean μ_t. VOLL is set to be \$2000/MWh, which is reasonable as the typical range of VOLL is between \$2000/MWh and \$50 000/MWh [20].

A. Probability Mass Function of Probabilistic LMP

Probability mass function of LMP_t at Bus B at two representing forecasted load levels, 730 MW and 900 MW, is calculated and shown in Table II. The same results are presented as a pie chart in Fig. 7. The results discover the fact that the deterministic LMP with respect to D_t^F may or may not be the price with the highest probability. For example, when forecasted load is 900 MW, the corresponding deterministic LMP is \$23.68/MWh and has the highest probability of 92.21%. However, the deterministic LMP \$21.74/MWh for forecasted load 730 MW has only the second highest probability of 32.80%, less than the probability of 36.29% for \$23.68/MWh. It shows that the deterministic LMP associated with the mean value of actual load does not necessarily bear the biggest probability. It should be noted that the price \$28.18/MWh is listed before \$26.38/MWh simply because this is the trend of price at Bus B when load grows. This is also shown with the gray boxes in Table I.

Table II and Fig. 7 can be very useful for buyer and sellers to develop bidding strategies, demand response offers, and even long-term contracts, since the results reveal the likelihood of

TABLE II
PMF OF LMP_t FOR BUS B

LMP($/MWh)	Probability(%) when D^F_t=730MW	Probability(%) when D^F_t =900MW
0	0.00	0.00
10	0.02	0.00
14	0.67	0.00
15	30.23	0.00
21.74	32.80	0.02
23.68	36.29	92.21
28.18	0.00	7.77
26.38	0.00	0.00
2000	0.00	0.00
Total	100	100

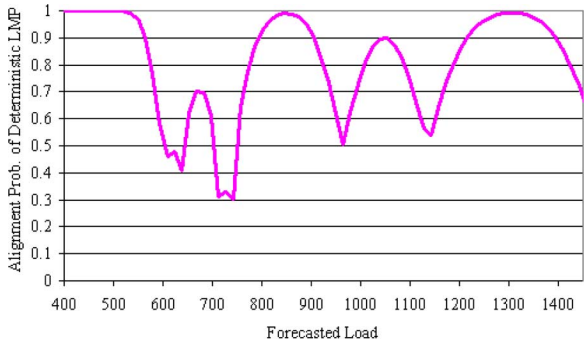

Fig. 8. Alignment probability of deterministic LMP at Bus B versus forecasted load.

realizing the forecasted LMP considering the fact that there is always certain error in the load forecast result.

Sometimes Fig. 7 may look messy when there are quite a few price candidates with considerable probability. In this case, it would be convenient to classify the prices into several groups. Depending on the strategies, planners or decision makers may also care more about the probability of a range of LMP, instead of any individual LMP. For example, a planner may group all the possible prices into three categories, $0 \leq \mathrm{LMP} \leq 15, 15 < \mathrm{LMP} < 30, 30 \leq \mathrm{LMP}$. The corresponding probabilities for each of the groups are 30.92%, 69.09%, 0% for forecasted load 730 MW, and 0%, 100%, 0% for forecasted load 900 MW.

B. Alignment Probability of Deterministic LMP

Fig. 8 shows the curve of alignment probability of deterministic LMP at Bus B versus forecasted load. By comparing Fig. 8 with Fig. 1, we can see that the low probabilities occur near CLLs, and the lowest probability is around 30%, indicating little confidence in the occurrence of the deterministic forecasted LMP. When forecasted load is over 1300 MW, the probability keeps decreasing as the forecasted load is approaching the maximum level (i.e., price of VOLL) that the system can afford, namely, 1484.06 MW.

Fig. 9 shows the alignment probability with 10% price tolerance. Taking Table II as an example, without tolerance, the

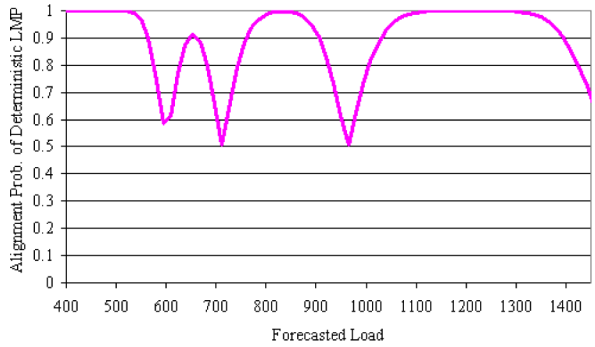

Fig. 9. Alignment probability of deterministic LMP at Bus B versus forecasted load (with 10% price tolerance).

TABLE III
EXPECTED VALUE OF PROBABILISTIC LMP IN COMPARISON WITH DETERMINISTIC LMP FOR BUS B

D^F_t(MW)	Expected Value of Probabilistic LMP($/MWh)	Deterministic LMP($/MWh)
730	20.35	21.74
900	24.03	23.68

alignment probability at 730 MW, where the deterministic LMP is $21.74/MWh, is 32.80% using (8). As a comparison, if 10% price tolerance is adopted, the alignment probability will be 69.09% $(= 32.80\% + 36.29\%)$ using (9).

As shown in Figs. 8 and 9, the alignment probability curve will be higher with 10% price tolerance, and the worst-case probability increases from 30% to 50%. Especially, the valley at around 1137 MW in Fig. 8 disappears in Fig. 9. The alignment probability at load 1137 MW is about 54% in Fig. 8, while it increases to nearly 99% with 10% price tolerance considered because in this case, the difference of deterministic LMP at CLL 1137.02 MW is within 10%.

C. Expected Value of Probabilistic LMP

The expected value of probabilistic LMP for the above case is compared with the deterministic LMP, $\mathrm{LMP}(D^F_t)$, which are shown in Table III. It shows that the expected value of probabilistic LMP can differ from the deterministic LMP for a specific forecasted load.

The expected value of probabilistic LMP versus forecasted load curve is shown in Fig. 10. Load range beyond 1350 MW is not shown simply because the high VOLL will make the curve not well-scaled to be illustrative. It should be noted that the expected LMP will escalate sharply when load is close to the maximum load level the system can afford, and will reach 2000 $/MWh eventually.

In the deterministic LMP-load curve in Fig. 1, the sensitivity for Bus E at 600 MW load level is mathematically infinite since a step change occurs at 600 MW. In the probability-based LMP-load curve, we know $\sum_{i=1}^{n} |p_i| = 2089$\$/MWh, $\mu_t = 600$ MW, $\sigma_t = 5\% \times \mu_t = 30$ MW; therefore, the upper bound of sensitivity is

$$\left| \frac{\partial E_{\mathrm{LMP}_t}(\mu_t, \sigma_t)}{\partial \mu_t} \right| \leq \frac{2089}{30\sqrt{2\pi}} = 27.78\ \$/\mathrm{MWh}^2.$$

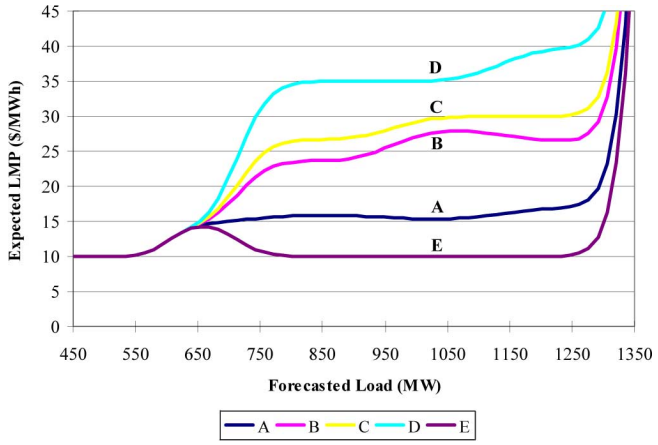

Fig. 10. Expected value of probabilistic LMP versus forecasted load.

Contrasted with the deterministic LMP-load curve in Fig. 1, the curve of expected value of probabilistic LMP in Fig. 10 demonstrates the same overall trend. However, Fig. 10 shows a much smoother curve without any step changes. This nice characteristic indicates that if the price simulation is based on the probabilistic approach described in this paper, the error or uncertainty with respect to the actual LMP in operation will be reduced because of the elimination of step changes as shown in Fig. 10. Hence, the planners will not face the 1-or-0 type of questions in their decision-making process when loads are around the CLLs. This continuous function, as well as the PMF function of probabilistic LMP shown in Table II and the alignment probability shown in Figs. 8 and 9, gives market-participating planners, forecasters, or decision-makers a better idea about the potential risk due to the uncertainty in load forecasting. So they can better evaluate the bidding strategies, demand offers, and forward contracts.

Also shown in this probabilistic LMP forecasting figure is that when the load is closer to CLLs, price uncertainty, i.e., the uncertainty associated with the forecasted deterministic LMP, will be higher. This matches the overall trend in the deterministic LMP in Fig. 1.

D. Impact of Load Forecasting Accuracy

In this subsection, three different levels of standard deviation of load forecasting are examined, 5%, 3%, and 1%. Fig. 11 shows the probabilities of all possible values of LMP_t at Bus B for these three levels of standard deviation when system load is 730 MW. It can be seen from Fig. 11 that the probability of realizing 21.74 $/MWh, the deterministic LMP at 730 MW load level, increases considerably with smaller standard deviation. This is reasonable because more accurate load forecast should lead to less deviation in forecasted price.

Fig. 12 compares the expected value of probabilistic LMP curves at the same bus. When forecasted load is quite away from any CLL, for example at 850 MW, the three curves overlap very well. It suggests different levels of standard deviation make trivial differences on expected LMP at this load level. In addition, the sensitivity of expected LMP at this load level is small, which indicates the expected LMP remains nearly constant when forecasted load varies slightly around

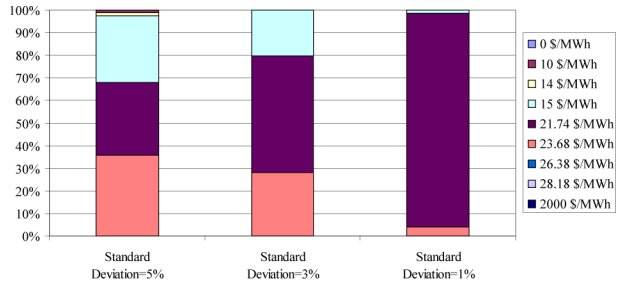

Fig. 11. PMF of LMP_t at Bus B for three levels of standard deviation when system load is 730 MW.

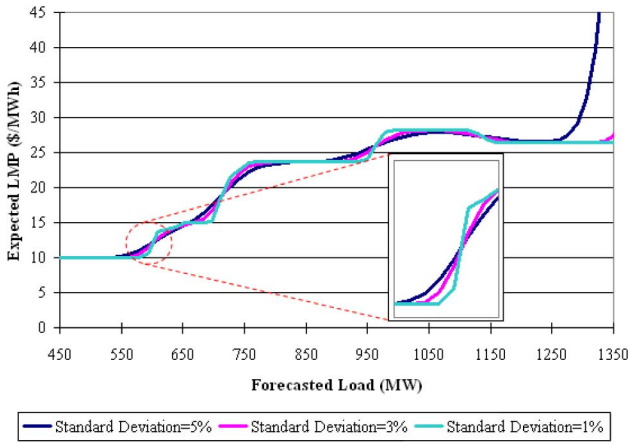

Fig. 12. Expected value of probabilistic LMP at Bus B versus forecasted load for three levels of standard deviation.

this level. In contrast, when forecasted load is close to a CLL, for example at 600 MW, the less the standard deviation is, the closer the curve is to a step change curve shape. Furthermore, the inset in Fig. 12 shows when the load level is closer to a CLL, the absolute value of sensitivity of expected LMP grows rapidly and expected LMP becomes more sensitive to variation of forecasted load.

V. Numerical Study of the IEEE 118-Bus System

The study results on the IEEE 118-bus system [21] are briefly presented in this section to demonstrate the applicability of the proposed concepts and methods to larger systems, while similar conclusions can be drawn as those for the PJM five-bus system. The system consists of 118 buses, 54 generators, and 186 branches. System total load is 4242 MW with 9966.2 MW total generation capacity. Detailed system data and diagram can be found in [21].

In the original IEEE 118-bus system, there is no generator bidding data and branch thermal limit data, which are indispensable to perform the study. Therefore, generator bidding data are assumed as follows for illustrative purpose: 20 cheap generators with bidding from $10 to $19.5 with $0.5 increment; 20 expensive generators with bidding from $30 to $49 with $1 increment; and 14 most expensive generators with bidding from $70 to $83 with $1 increment. Five thermal limits are added into the transmission system: 345 MW for line 69–77, 630 MW for line 68–81, 106 MW for line 83–85 and 94–100, 230 MW for line 80–98. VOLL is set to be 2000 $/MWh for all loads.

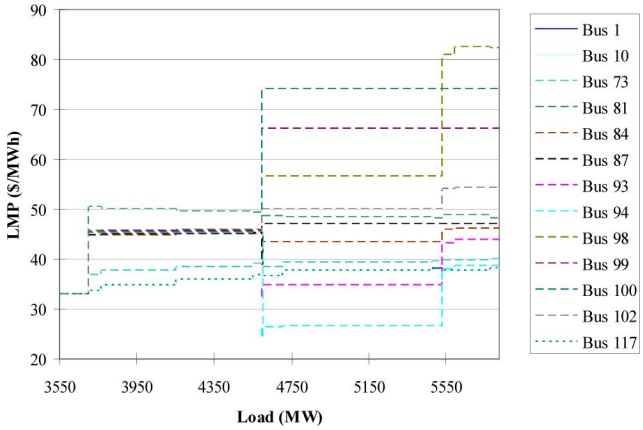

Fig. 13. Deterministic LMP curve at selected buses with respect to different system loads for the IEEE 118-bus system.

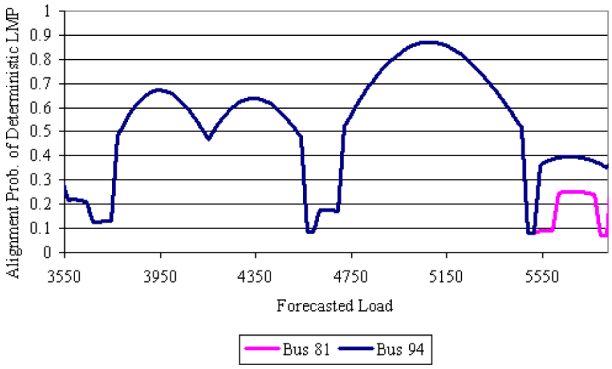

Fig. 14. Alignment probability of deterministic LMP at Bus 81 and Bus 94 versus forecasted load for the IEEE 118-bus system.

The deterministic LMP versus load curve for the IEEE 118-bus system is shown in Fig. 13. For better illustration, the curves are drawn only for a few selected buses and in a broad neighborhood of base case load, namely, from 3550 MW to 5820 MW. Once again, the step change characteristic of the deterministic LMP curves is observed in Fig. 13.

Fig. 14 shows the curve of alignment probability of deterministic LMP at two selected buses versus forecasted load. The locations where low probabilities occur are aligned with the CLLs very well, because the step changes of deterministic LMP contribute to the price uncertainty when load forecast errors are present. In Fig. 14, majority of the alignment probability is less than 70%, and only a small range of load (around 4920 MW–5230 MW) carries an 80% or more probability for realizing the deterministic forecasted LMP. Compared to smaller system results as in Fig. 8, larger systems tend to have lower overall alignment probability since there are more CLLs or narrower ranges among two consecutive CLLs because there are more generators and potentially more congested lines are involved.

It can be seen from Fig. 14 that alignment probabilities for Bus 81 and Bus 94 are almost identical for a vast load range (3550 MW–5538 MW). This is because the price changes at these two buses synchronize with load changes very well. This is a common pattern because the LMP at any specific bus will

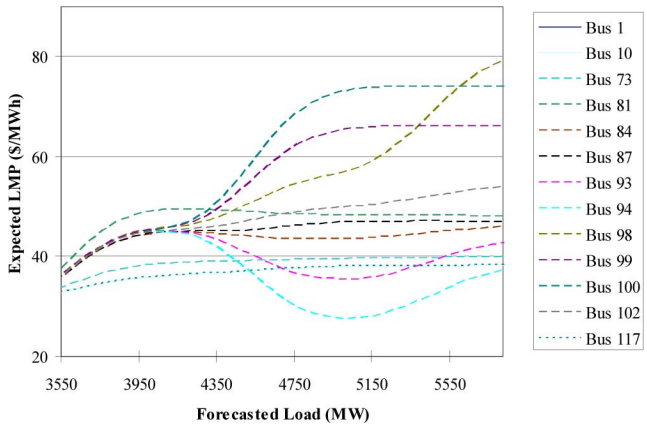

Fig. 15. Expected value of probabilistic LMP at selected buses versus forecasted load for the IEEE 118-bus system.

change at CLLs unless there is a marginal unit at that bus to keep the LMP remaining unchanged.

Fig. 15 presents the expected value of probabilistic LMP versus forecasted load curve at the same selected buses as in Fig. 13. The curves are observed to be highly smooth and there is no step change. Meanwhile, the curves track the overall trend of their deterministic counterparts. It should be noted that skyrocketing pattern in the right part of Fig. 10 for the PJM five-bus system is not present in Fig. 15, because the load window shown in Fig. 15 is quite distant from the maximum affordable load. Therefore, VOLL does not have any impact on this load range of interest.

VI. Conclusion

Load uncertainty exists due to a variety of reasons. Meanwhile, the LMP-load curve has step changes at critical load levels where a new binding limit occurs. These are the major reasons of LMP uncertainty. This paper studies the LMP uncertainty with respect to load in a probabilistic sense. The contribution can be summarized as follows:

- With the assumption of normal distribution of actual load, the concept of probabilistic LMP is proposed and its probability mass function at hour t is presented. The probabilistic LMP does not correspond to a single deterministic value. Instead, it represents a set of discrete values $(\{p_i\}_{i=0}^{n})$ at a number of load intervals, and each value p_i has an associated probability.
- Alignment probability is proposed and formulated to define the likelihood that the actual LMP is the same as (or within a tolerance level of) the deterministic LMP calculated based on a single value of forecasted load. The alignment probability curve delivers the information of how likely the result from the deterministic LMP is acceptable.
- The expected value of probabilistic LMP is derived and its curve with respect to forecasted load is presented. The sensitivity of the curve is derived and shown to be bounded by finite values. In addition, the expected value of probabilistic LMP versus forecasted load curve is smooth and has no step changes. This avoids the 0-or-1 type of step changes if deterministic LMP forecast is performed, and

helps market participants make less risky decisions in generation bidding, demand offers, and/or forward contract negotiation.

The proposed concept and method are illustrated on a modified PJM five-bus system as well as the IEEE 118-bus system. The results provide additional and useful information for understanding the LMP-load curve from a probabilistic perspective.

Possible future work may include the consideration of loss of the system and more sophisticated load variation model.

APPENDIX

A. Derivation of (13)

Equation (12) can be further decomposed into several parts:

$$\begin{aligned}
&\frac{\partial E_{\mathrm{LMP}_t}(\mu_t,\sigma_t)}{\partial \mu_t}\\
&\quad=\sum_{i=0}^{n} p_i \times \int_{D_i}^{D_{i+1}} \frac{u-\mu_t}{\sigma_t^3\sqrt{2\pi}} e^{-\frac{(u-\mu_t)^2}{2\sigma_t^2}}\,du\\
&\quad= p_0 \times \int_{D_0}^{D_1} \frac{u-\mu_t}{\sigma_t^3\sqrt{2\pi}} e^{-\frac{(u-\mu_t)^2}{2\sigma_t^2}}\,du\\
&\qquad+\sum_{i=1}^{n-1} p_i \times \int_{D_i}^{D_{i+1}} \frac{u-\mu_t}{\sigma_t^3\sqrt{2\pi}} e^{-\frac{(u-\mu_t)^2}{2\sigma_t^2}}\,du\\
&\qquad+ p_n \times \int_{D_n}^{D_{n+1}} \frac{u-\mu_t}{\sigma_t^3\sqrt{2\pi}} e^{-\frac{(u-\mu_t)^2}{2\sigma_t^2}}\,du\\
&\quad=\sum_{i=1}^{n-1} p_i \times \int_{D_i}^{D_{i+1}} \frac{u-\mu_t}{\sigma_t^3\sqrt{2\pi}} e^{-\frac{(u-\mu_t)^2}{2\sigma_t^2}}\,du\\
&\qquad+ p_n \times \int_{D_n}^{D_{n+1}} \frac{u-\mu_t}{\sigma_t^3\sqrt{2\pi}} e^{-\frac{(u-\mu_t)^2}{2\sigma_t^2}}\,du. \qquad \text{(A1)}
\end{aligned}$$

Each integration of (A1) can be solved as follows:

$$\begin{aligned}
&\int_{D_i}^{D_{i+1}} \frac{u-\mu_t}{\sigma_t^3\sqrt{2\pi}} e^{-\frac{(u-\mu_t)^2}{2\sigma_t^2}}\,du\\
&\quad=\frac{1}{\sigma_t^3\sqrt{2\pi}} \int_{D_i}^{D_{i+1}} (u-\mu_t)\times e^{-\frac{(u-\mu_t)^2}{2\sigma_t^2}}\,du\\
&\quad=\frac{1}{\sigma_t^3\sqrt{2\pi}} \int_{D_i}^{D_{i+1}} \left(-\frac{1}{2}\right)\times e^{-\frac{(u-\mu_t)^2}{2\sigma_t^2}} \times d(-(u-\mu_t)^2)\\
&\quad=\frac{1}{\sigma_t^3\sqrt{2\pi}} \int_{D_i}^{D_{i+1}} (-\frac{1}{2})\times 2\sigma_t^2\\
&\qquad\times e^{-\frac{(u-\mu_t)^2}{2\sigma_t^2}} d\left(-\frac{(u-\mu_t)^2}{2\sigma_t^2}\right)\\
&\quad=-\frac{1}{\sigma_t\sqrt{2\pi}} \int_{D_i}^{D_{i+1}} e^{-\frac{(u-\mu_t)^2}{2\sigma_t^2}} d\left(-\frac{(u-\mu_t)^2}{2\sigma_t^2}\right)\\
&\quad=-\frac{1}{\sigma_t\sqrt{2\pi}} e^{-\frac{(u-\mu_t)^2}{2\sigma_t^2}}\Bigg|_{D_i}^{D_{i+1}}\\
&\quad=\frac{1}{\sigma_t\sqrt{2\pi}}\left(e^{-\frac{(D_i-\mu_t)^2}{2\sigma_t^2}} - e^{-\frac{(D_{i+1}-\mu_t)^2}{2\sigma_t^2}}\right). \qquad \text{(A2)}
\end{aligned}$$

Specifically, when $i=n$, (A2) can be further derived as

$$\begin{aligned}
&\int_{D_i}^{D_{i+1}} \frac{u-\mu_t}{\sigma_t^3\sqrt{2\pi}} e^{-\frac{(u-\mu_t)^2}{2\sigma_t^2}}\,du\\
&\quad=\int_{D_n}^{D_{n+1}} \frac{u-\mu_t}{\sigma_t^3\sqrt{2\pi}} e^{-\frac{(u-\mu_t)^2}{2\sigma_t^2}}\,du\\
&\quad=\int_{D_n}^{\infty} \frac{u-\mu_t}{\sigma_t^3\sqrt{2\pi}} e^{-\frac{(u-\mu_t)^2}{2\sigma_t^2}}\,du\\
&\quad=\frac{1}{\sigma_t\sqrt{2\pi}} e^{-\frac{(D_n-\mu_t)^2}{2\sigma_t^2}}. \qquad \text{(A3)}
\end{aligned}$$

Plugging (A2) and (A3) into (A1), we have the formula of sensitivity of expected value of probabilistic LMP

$$\begin{aligned}
&\frac{\partial E_{\mathrm{LMP}_t}(\mu_t,\sigma_t)}{\partial \mu_t}\\
&\quad=\sum_{i=1}^{n-1} p_i \times \int_{D_i}^{D_{i+1}} \frac{u-\mu_t}{\sigma_t^3\sqrt{2\pi}} e^{-\frac{(u-\mu_t)^2}{2\sigma_t^2}}\,du\\
&\qquad+ p_n \times \int_{D_n}^{D_{n+1}} \frac{u-\mu_t}{\sigma_t^3\sqrt{2\pi}} e^{-\frac{(u-\mu_t)^2}{2\sigma_t^2}}\,du\\
&\quad=\sum_{i=1}^{n-1} p_i \times \frac{1}{\sigma_t\sqrt{2\pi}}\left(e^{-\frac{(D_i-\mu_t)^2}{2\sigma_t^2}} - e^{-\frac{(D_{i+1}-\mu_t)^2}{2\sigma_t^2}}\right)\\
&\qquad+ p_n \times \frac{1}{\sigma_t\sqrt{2\pi}} e^{-\frac{(D_n-\mu_t)^2}{2\sigma_t^2}}\\
&\quad=\frac{1}{\sigma_t\sqrt{2\pi}} \times \left[\sum_{i=1}^{n-1} p_i \times \left(e^{-\frac{(D_i-\mu_t)^2}{2\sigma_t^2}}\right.\right.\\
&\qquad\left.\left.-e^{-\frac{(D_{i+1}-\mu_t)^2}{2\sigma_t^2}}\right) + p_n \times e^{-\frac{(D_n-\mu_t)^2}{2\sigma_t^2}}\right]. \qquad \text{(A4)}
\end{aligned}$$

The last step of (A4) gives (13).

B. Derivation of (14)

Based on (13), the bounds of the sensitivity of expected value of probabilistic LMP can be obtained as follows:

$$\begin{aligned}
&\left|\frac{\partial E_{\mathrm{LMP}_t}(\mu_t,\sigma_t)}{\partial \mu_t}\right|\\
&\quad=\left|\frac{1}{\sigma_t\sqrt{2\pi}} \times \left(\sum_{i=1}^{n-1} p_i \times \left(e^{-\frac{(D_i-\mu_t)^2}{2\sigma_t^2}}\right.\right.\right.\\
&\qquad\left.\left.\left.-e^{-\frac{(D_{i+1}-\mu_t)^2}{2\sigma_t^2}}\right) + p_n \times e^{-\frac{(D_n-\mu_t)^2}{2\sigma_t^2}}\right)\right|\\
&\quad\le \frac{1}{\sigma_t\sqrt{2\pi}} \times \left(\left|\sum_{i=1}^{n-1} p_i \times \left(e^{-\frac{(D_i-\mu_t)^2}{2\sigma_t^2}}\right.\right.\right.\\
&\qquad\left.\left.\left.-e^{-\frac{(D_{i+1}-\mu_t)^2}{2\sigma_t^2}}\right)\right| + \left|p_n \times e^{-\frac{(D_n-\mu_t)^2}{2\sigma_t^2}}\right|\right)\\
&\quad\le \frac{1}{\sigma_t\sqrt{2\pi}} \times \left(\sum_{i=1}^{n-1} |p_i|\times 1 + |p_n|\times 1\right)\\
&\quad\le \frac{1}{\sigma_t\sqrt{2\pi}} \sum_{i=1}^{n} |p_i|. \qquad \text{(B1)}
\end{aligned}$$

The last step in (B1) gives (14).

REFERENCES

[1] G. Gross and F. D. Galiana, "Short-term load forecasting," *Proc. IEEE*, vol. 75, no. 12, pp. 1558–1573, Dec. 1987.

[2] J. Bastian, J. Zhu, V. Banunarayanan, and R. Mukerji, "Forecasting energy prices in a competitive market," *IEEE Comput. Appl. Power Mag.*, vol. 12, no. 3, pp. 40–45, Jul. 1999.

[3] G. Li, C.-C. Liu, C. Mattson, and J. Lawarree, "Day-ahead electricity price forecasting in a grid environment," *IEEE Trans. Power Syst.*, vol. 22, no. 1, pp. 266–274, Feb. 2007.

[4] P. Mandal, T. Senjyu, N. Urasaki, T. Funabashi, and A. K. Srivastava, "A novel approach to forecast electricity price for PJM using neural network and similar days method," *IEEE Trans. Power Syst.*, vol. 22, no. 4, pp. 2058–2065, Nov. 2007.

[5] K. Xie, Y.-H. Song, J. Stonham, E. Yu, and G. Liu, "Decomposition model and interior point methods for optimal spot pricing of electricity in deregulation environments," *IEEE Trans. Power Syst.*, vol. 15, no. 1, pp. 39–50, Feb. 2000.

[6] F. Li and R. Bo, "DCOPF-based LMP simulation: Algorithm, comparison with ACOPF, and sensitivity," *IEEE Trans. Power Syst.*, vol. 22, no. 4, pp. 1475–1485, Nov. 2007.

[7] J. E. Price, "Market-based price differentials in zonal and LMP market designs," *IEEE Trans. Power Syst.*, vol. 22, no. 4, pp. 1486–1494, Nov. 2007.

[8] D. K. Ranaweera, G. G. Karady, and R. G. Farmer, "Economic impact analysis of load forecasting," *IEEE Trans. Power Syst.*, vol. 12, no. 3, pp. 1388–1392, Aug. 1997.

[9] J. Valenzuela, M. Mazumdar, and A. Kapoor, "Influence of temperature and load forecast uncertainty on estimation of power generation production costs," *IEEE Trans. Power Syst.*, vol. 15, no. 2, pp. 668–674, May 2000.

[10] R. Billinton and D. Huang, "Effects of load forecast uncertainty on bulk electric system reliability evaluation," *IEEE Trans. Power Syst.*, vol. 23, no. 2, pp. 418–425, May 2008.

[11] M. A. Ortega-Vazquez and D. S. Kirschen, "Economic impact assessment of load forecast errors considering the cost of interruptions," in *Proc. 2006 IEEE Power Eng. Soc. General Meeting*, Montréal, QC, Canada, 2006.

[12] H. Wang, C. E. Murillo-Sanchez, R. D. Zimmerman, and R. J. Thomas, "On computational issues of market-based optimal power flow," *IEEE Trans. Power Syst.*, vol. 22, no. 3, pp. 1185–1193, Aug. 2007.

[13] A. J. Conejo, E. Castillo, R. Minguez, and F. Milano, "Locational marginal price sensitivities," *IEEE Trans. Power Syst.*, vol. 20, no. 4, pp. 2026–2033, Nov. 2005.

[14] F. Li, "Continuous locational marginal pricing (CLMP)," *IEEE Trans. Power Syst.*, vol. 22, no. 4, pp. 1638–1646, Nov. 2007.

[15] F. Li and R. Bo, "Congestion and price prediction under load variation," *IEEE Trans. Power Syst.*, vol. 24, no. 2, pp. 911–922, May 2009.

[16] PJM, *PJM Training Materials (LMP101).* [Online]. Available: http://www.pjm.com/services/training/train-materials.html.

[17] Y. He and Y. H. Song, "Integrated biding strategies by optimal response to probabilistic locational marginal prices," *Proc. Inst. Elect. Eng., Gen., Transm., Distrib.*, vol. 149, no. 6, pp. 633–639, Nov. 2002.

[18] X. Chen *et al.*, "Study of impacts of physical contracts and financial contracts on bidding strategies of GENCOs," *Elect. Power Energy Syst.*, vol. 26, pp. 715–723, 2004.

[19] M. Abramowitz and I. Stegun, *Handbook of Mathematical Functions with Formulas, Graphs, and Mathematical Tables*. New York: Dover, 1964.

[20] J. Yang, "Resource adequacy: Economic and engineering challenges and proposed solutions," *IEEE Power Energy Mag.*, vol. 4, no. 2, pp. 59–65, Mar.–Apr. 2006.

[21] Univ. Washington, *Power System Test Case Archive*. [Online]. Available: http://www.ee.washington.edu/research/pstca/.

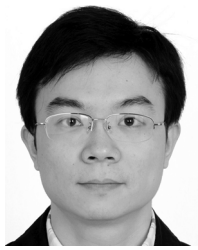

Rui Bo (S'02) received the B.S. and M.S. degrees in electric power engineering from Southeast University of China, Nanjing, China, in 2000 and 2003, respectively. He is pursuing the Ph.D. degree at The University of Tennessee, Knoxville.

From 2003 to 2005, he worked at ZTE Corporation and Shenzhen Cermate, Inc., respectively. His current interests include power system operation and planning, power system economics, and market simulation.

Fangxing (Fran) Li (M'01–SM'05) received the B.S. and M.S. degrees in electric power engineering from Southeast University, Nanjing, China, in 1994 and 1997, respectively, and the Ph.D. degree from Virginia Tech, Blackburg, in 2001.

He has been an Assistant Professor at The University of Tennessee (UT), Knoxville, since August 2005. Prior to joining UT, he was a Principal Engineer at ABB Electrical System Consulting (ESC). During his 4.5 years of employment at ABB, he was the lead developer of GridView™, ABB's market simulation software tool. His current interests include energy market, reactive power, distributed energy resources, distribution systems, reliability, and computer applications.

Dr. Li is a member of Sigma Xi—The Scientific Research Society and a registered Professional Engineer (PE) in the state of North Carolina.